Polímeros
ISSN 1678-5169 (Online)

https://doi.org/10.1590/0104-1428.20240077

# Magnesium layered double hydroxide nanofiller in PMMA exposed to gamma irradiation

**Dandara Luz Souza de Oliveira[1] , Amanda Damasceno Leão[2], Fábio de Oliveira da Silva Ribeiro[3], Alyne Rodrigues de Araújo[3], Pietro Paolo Jorge Correia de Oliveira e Silva[4], José Lamartine Soares-Sobrinho[2], Elmo Silvano de Araújo[1], Renata Francisca da Silva Santos[1] and Kátia Aparecida da Silva Aquino[1]***

*[1]Departamento de Energia Nuclear, Universidade Federal de Pernambuco – UFPE, Recife, PE, Brasil*
*[2]Departamento de Ciências Farmacêuticas, Universidade Federal de Pernambuco – UFPE, Recife, PE, Brasil*
*[3]Centro de Pesquisa em Biodiversidade e Biotecnologia – BIOTEC, Universidade Federal do Delta do Parnaíba – UFDPar, Parnaíba, PI, Brasil*
*[4]Instituto Federal de Pernambuco – IFPE, Recife, PE, Brasil*
***aquino@ufpe.br***

## Abstract

Poly(methyl methacrylate) (PMMA) is a polymer that can be used in applications requiring its exposition to gamma radiation, nevertheless, the radiation induces main chain scission backbone, leading to modification in some properties. Therefore, using materials such as layered double hydroxide (LDH), was evaluated as a new radiation shielding agent. This work synthesized LDH and added to PMMA by an in-situ polymerization method. Viscosimetric analysis showed that LDH at 0.25 wt% concentration promotes polymer radiolytic protection of 90% against damage caused by gamma radiation. The topographic images obtained by AFM revealed increasing PMMA/LDH film roughness, which impacted the lower film transmittance. The combined effect of LDH and gamma radiation interferes with the degradation process of PMMA, promoting reduced rigidity, greater mobility of polymer chains, and lower optical gap energy. Thus, these results open a promising path for using LDH as additives in polymers exposed to gamma radiation.

**Keywords:** *gamma irradiation, layered double hydroxide, poly(methyl methacrylate), radiolytic protection.*

**Howe to cite:** Oliveira, D. L. S., Leão, A. D., Ribeiro, F. O. S., Araújo, A. R., Silva, P. P. J. C. O., Soares-Sobrinho, J. L., Araújo, E. S., Santos, R. F. S., & Aquino, K. A. S. (2025). Magnesium layered double hydroxide nanofiller in PMMA exposed to gamma irradiation. *Polímeros: Ciência e Tecnologia*, *35*(1), e20250001. https://doi.org/10.1590/0104-1428.20240077

## 1. Introduction

Layered Double Hydroxides (LDHs) are inorganic materials that have attracted attention due to their properties, such as large surface area, adsorption capacity, ion intercalation, and synthesis through various synthetic routes[1,2]. LDHs are considered an emerging class of nanofillers for preparing nanocomposites[3]. These compounds, also known as hydrotalcite, consist of lamellar inorganic sheets positively charged by cations such as $Zn^{2+}$ and $Mg^{2+}$, balanced by hydroxide ions and anions such as fluorides, chlorides, and carbonates. LDHs have received significant attention due to their various applications, considering their properties, composition, thermal stability, and other physicochemical parameters[4,5].

On the other hand, poly(methyl methacrylate) (PMMA) is a rigid thermoplastic polymer with excellent optical properties, easy processability, and good thermal and mechanical properties. Its use dates back to the 1930s in manufacturing removable prosthetics, orthodontic appliances, and splints that can be sterilized through exposure to gamma radiation. However, gamma radiation induces the scission of the polymer main chain[6]. In light of this, PMMA has been studied with commercial additives[7] and nanoparticles[8,9] to make the polymer resistant to gamma radiation.

Studies indicate that the PMMA/LDH nanocomposite can be obtained through various methods, such as sonication, LDH gel formation, reflux synthesis, and intercalation with dodecyl sulfate[3,10]. The recorded results demonstrate an enhancement of PMMA properties by incorporating zinc and magnesium LDH in small proportions[11]. One key feature that makes the PMMA/LDH system promising is the ease with which LDH can disperse in the polar polymeric matrix since PMMA[5,12].

However, in the sources analyzed thus far, no records have been found regarding the effects of gamma radiation exposure in systems composed of PMMA/LDH. PMMA produces displays, dental materials, and artifacts subjected to radiation sterilization[13-16]. Therefore, there is relevance in carrying out studies that investigate the influence of LDH on the radiolytic effects in the PMMA matrix. Consequently, there is a need to prospect new formulations in which LDH provides radiolytic protection to PMMA. Additionally, in this context, this study will analyze the changes that the PMMA/LDH nanocomposite may undergo when exposed to gamma radiation. Thus, this research may contribute to the field of materials science by providing insights into the interaction between radiation and the PMMA/LDH nanocomposite to enhance its utility in situations that require radiation resistance.

## 2. Materials and Methods

### 2.1 LDH and PMMA/LDH nanocomposites preparation

This study synthesized magnesium LDH using the constant pH co-precipitation method in an unheated methanolic solution as previously reported by our group[1,17,18].

The PMMA/LDH nanocomposites were produced through an in-situ polymerization reaction. Initially, the methyl methacrylate (MMA) monomer required a purification process as it typically contains inhibitors and water that can influence polymerization yield. MMA was washed with 5% (w/v) sodium hydroxide and distilled water. Subsequently, it was collected in a flask containing calcium chloride to remove inhibitors, filtered, and stored in a freezer for 12 hours at -15 °C to crystallize residual water. The crystallized water was removed, and pure MMA was used in the polymerization reaction. The benzoyl peroxide (BPO) initiator was purified by solubilizing it in chloroform (30 µg/mL), precipitating it in methanol, and storing it at -15 °C. The crystals were filtered and dried in an oven at 40 °C until reaching a constant weight[2].

In a typical in situ polymerization procedure for PMMA, 9.36 g of MMA monomer was mixed with 0.096 g of BPO initiator, and the resulting system was shaken in an orbital shaker for 2 hours at 80 °C. The nanocomposite systems were removed from the shaker and kept at room temperature for 24 hours to complete the polymerization reaction. For nanocomposite preparation, the appropriate amount of LDH was dispersed in the monomer, stirring for 20 minutes at room temperature (≈ 25 °C) before adding BPO. PMMA/LDH systems were obtained at 0.25, 0.5, 1.0, and 2.0 wt% concentrations.

The PMMA/LDH nanocomposites and the synthesized PMMA were dissolved in 20 mL of methyl ethyl ketone (MEK) under magnetic stirring for 24 hours at room temperature. Then, the films were obtained by casting method in an oven at 45 °C for 4 hours[2,17].

### 2.2 Films irradiation

PMMA and PMMA/LDH films were irradiated with gamma rays from a $^{60}$Co source (dose rate of 4.606 kGy/h) at 25 kGy (sterilization dose). The sample irradiations were carried out in ambient air at room temperature.

### 2.3 Viscosimetric analysis

Solutions of 10 mL were produced in triplicate at 0.6 g/dL of concentration with PMMA and PMMA/LDH films (irradiated and non-irradiated). The kinematic viscosity of the solutions ($\nu$) and the solvent ($\nu_0$) were determined at 25 °C using a Stabinger Anton Paar SVM 3000/G2s viscometer. The relative ($\eta_r$), specific ($\eta_{sp}$), reduced ($\eta_{red}$), and intrinsic ($[\eta]$) viscosities were obtained using the kinematic viscosity through the equations described in Table S1 (Supplementary Material)[5,6,19-27]. The value of $[\eta]$ was used to obtain the viscosity molar mass ($M_v$) using the Mark-Houwink-Sakurada relationship (Equation 1)[28].

$$\left[\eta\right] = KM_v^a \quad (1)$$

K and *a* are 0.72 and 6.8 x $10^{-5}$ (dL/g), respectively, for the PMMA/MEK system, at 25 °C[29]. From the viscosity molar mass values before ($M_{vo}$) and after ($M_v$) irradiation, the degradation index ( $ID = \left(\frac{M_{vo}}{M_v}\right) - 1$ ) and the protection degree $\left(P = \left(\frac{ID_o - ID}{ID_o}\right) x100\right)$ where calculated.

### 2.4 Spectroscopic tests

Infrared spectra were acquired using the FT-IR Jasco Spectrophotometer, model 4600, with 32 scans, a resolution of 4 $cm^{-1}$, in transmission mode within the range of 4000-400 $cm^{-1}$, employing the Attenuated Total Reflectance (ATR) technique.

UV-vis spectra were obtained using the UV-vis Spectrophotometer Jasco, model V-730, covering the absorption range from 200 to 800 nm. From the absorption edge (A), determined by the position of the maximum absorption band in the spectrum, it was possible to ascertain the optical parameters of the films since their absorption coefficient ($\alpha$) depends on the frequency of the absorbed photon ($\nu$) and can be defined by the Beer-Lambert law[5] as shown in Equations S1-S9 (Supplementary Material).

### 2.5 Mechanical properties

Mechanical tensile testing was carried out on three samples from each system on an Instron IMIC machine, 500 N, with a 2 mm/s crosshead speed. The ASTM-D822 standard was used with films measuring 7.5 × 2.5 cm. The results were expressed as average ± standard deviation, and a $p$-value $< 0.05$ was considered statistically significant after the Tukey test. The mechanical properties analyzed were tensile stress (MPa), Young modulus (MPa), and elongation at break (mm).

### 2.6 Scanning electron microscopy

Scanning Electron Microscopies (SEM) were obtained using HITACHI equipment, model TM3000, with an acceleration voltage of 15 kV. Using plasma in an argon atmosphere, the samples were metalized with gold in a Quorum QI50R metallizer for 30 s at 20 mA.

### 2.7 Atomic force microscopy

The morphological analysis of the films was carried out by Atomic Force Microscopy (AFM) in TT-AFM equipment (AFM Workshop, USA), in intermittent contact mode (vibrating), with a resolution of 512 × 512 pixels, using TAP300-G silicon probes (Ted Pella, USA), with a resonance frequency of approximately 247 kHz. The images were examined using the Gwyddion 2.59 program, from which the average roughness values were extracted. Statistical analyses were performed using the GraphPad Prism® 8.0.1 program, using one-way ANOVA with Tukey's post-test. The results were expressed as average ± standard error of the mean, and a p-value <0.05 was considered statistically significant.

## 3. Results and Discussions

### *3.1 Viscosimetric tests*

Figure S1 (Supplementary Material) shows a micrograph (x50,000) of the magnesium LDH synthesized for this study. LDH presented a flat surface morphology with platelets with irregular edges and an average size of 100 to 200 nm in the horizontal axis. The results of the complete characterization of the magnesium LDH and the synthesized PMMA were recorded in our previous work[11].

The PMMA and PMMA/LDH films, obtained by the casting method, exhibited a homogeneous appearance, with an average thickness of 0.112 ± 0.002 mm. No change in film thickness was recorded with the addition of LDH to the system.

For the viscosimetric tests, initially, the Huggins constant (Kh) was calculated to find out which equation would be most suitable for obtaining the intrinsic viscosity ([η]) by a single-point method. Figure S2 (Supplementary Material) shows the relationship between the concentrations of non-irradiated PMMA solutions and their respective reduced viscosities by the Huggins model[20].

The Kh = 0.49 was calculated using the obtained straight-line equation of Figure S2, indicating the Solomon-Ciuta equation (see Table S1 in Supplementary Material) to get the intrinsic viscosity by a single-point method. Table 1 shows the viscosimetric results obtained for the systems under study.

When comparing the Mv values of non-irradiated systems, the values of systems with LDH are slightly lower than those of pure PMMA. These results highlight the influence of LDH on the PMMA matrix. Typically, the PMMA molecule exhibits dipole-dipole attraction due to electrostatic interactions between the oxygen atom of the ester group in a polymer chain (negative pole) and the hydrogen atom of another polymer molecule (positive pole). For example, LDH molecules may induce contraction of PMMA molecules due to a lack of chemical affinity. Thus, the contracted coil of PMMA/LDH systems results in a smaller hydrodynamic volume, facilitating the passage of the polymeric solution through the capillary tube of the viscometer and reducing its intrinsic viscosity, as shown in Table 1[30].

On the other hand, when analyzing the irradiated systems, Mv values are lower than those of non-irradiated systems. The decrease in Mv is attributed to the scission of the main chain of PMMA, a well-established mechanism[6,31]. Pure PMMA exhibited a reduction in Mv of approximately 31.5%. Unlike those with lower concentrations, the PMMA/LDH systems at concentrations of 1 and 2 wt% showed a decrease in Mv very close to PMMA, with a modest percentage of radiolytic protection.

The PMMA/LDH system at a concentration of 0.25 wt% exhibited an ID of 0.05, and the system with a concentration of 0.5% (w/w) showed an ID of 0.09. In other words, these systems reduced radiolytic degradation effects. Compared to the ID of pure PMMA (ID=0.46), protection of over 80% from LDH against the chain scission effects caused by gamma radiation exposure was calculated. PMMA undergoes radiolytic degradation by a radical mechanism [6]. Therefore, it was inferred that LDH acts as a scavenger agent, preventing the action of radicals formed in the radiolysis process.

Based on the results presented thus far, the sample that demonstrated the best performance in radioprotective action for PMMA was the one with LDH at a concentration of 0.25 wt%. The reduction in the protection factor in systems with higher concentrations of LDH indicates that, as the amount of LDH in the system increases, an impurity-like behavior establishes itself, competing with its radioprotective action. Similar outcomes were found in other studies employing PMMA and additives with radioprotective properties[8,9,32,33]. Consequently, the following sections will show characterization results for the PMMA/LDH system at a concentration of 0.25 wt%.

### *3.2 AFM and SEM*

Figure 1 shows topographic images of irradiated and non-irradiated PMMA and PMMA/LDH (0.25 wt%) films. The 2D-amplitude image of the non-irradiated PMMA film exhibits a flatter and more homogeneous surface when compared to the PMMA/LDH samples, which show a globular

**Table 1.** Viscosimetric results of PMMA and PMMA/LDH films.

| Dose (kGy) | LDH Concentration (% wt)) | [η] dL/g | $M_v$ ± SD (x $10^4$) (g/mol) | ID | Protection (%) |
|---|---|---|---|---|---|
| 0 | 0 | 0.54 ± 0.01 | 26.41 ± 0.56 | | - |
| 25 | | 0.42 ± 0.02 | 18.09 ± 0.12 | 0.46 | |
| 0 | 0.25 | 0.46 ± 0.01 | 19.97 ± 0.10 | | |
| 25 | | 0.45 ± 0.02 | 19.06 ± 0.31 | 0.05 | 89.61 |
| 0 | 0.5 | 0.53 ± 0.01 | 25.55 ± 0.57 | | |
| 25 | | 0.49 ± 0.02 | 23.53 ± 0.18 | 0.09 | 81.36 |
| 0 | 1 | 0.51 ± 0.02 | 24.14 ± 0.16 | | |
| 25 | | 0.38 ± 0.01 | 17.04 ± 0.22 | 0.42 | 9.10 |
| 0 | 2 | 0.52 ± 0.04 | 24.37 ± 0.46 | | |
| 25 | | 0.40 ± 0.03 | 17.33 ± 0.82 | 0.41 | 11.48 |

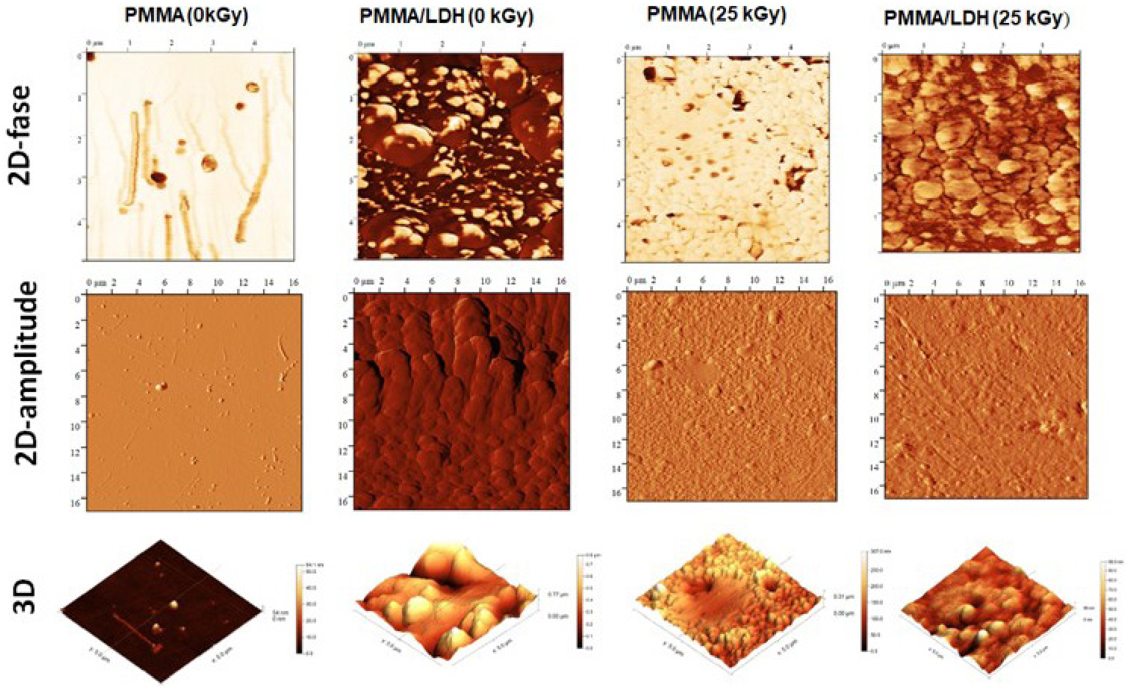

**Figure 1.** Topographic images of PMMA and PMMA/LDH (0.25 wt%), irradiated and non-irradiated samples, with a resolution of 512×512 pixels.

surface due to the lateral spreading of the LDH lamellae. On the other hand, for irradiated PMMA and PMMA/LDH films, the formation of fragments corresponds to the degradation process induced by gamma radiation. This action is better observed in the 2D-phase image when comparing irradiated and non-irradiated films. For the PMMA samples, the 2D-phase images show some polymer aggregates, while the irradiated sample displays fragmentation of the aggregates with a higher number of pores, likely obtained due to chain scission in the polymer caused by radiation [6]. For the PMMA/LDH films, delaminated LDH lamellae are observed against a continuous background of PMMA, with no significant difference between the samples except for a reduced aggregate size.

In the 3D-phase images, the behavior of the film surfaces can be better observed. When irradiated, PMMA exhibits the formation of pores and increased roughness. The average roughness value for PMMA is 2.51 ± 0.29 nm, which rises to 13.36 ± 0.89 nm in irradiated films, representing a difference of 10.85 nm according to the Tukey test (p=0.0018). This result highlights the extent of radiation-induced damage to the PMMA matrix.

The 3D images also reveal that PMMA/LDH films are rougher than irradiated PMMA films. However, radiation has the opposite effect on PMMA/LDH systems. The roughness of the irradiated PMMA/LDH becomes lower than the non-irradiated film. The average roughness value for the non-irradiated PMMA/LDH is 57 ± 4 nm, while 11 ± 1 nm was found for the irradiated film. According to the Tukey test, this result signifies a decrease of 46 nm (p=0.001). Although the roughness of LDH-containing samples decreased with irradiation, no pores were observed in the irradiated film, which may be associated with the protective effect of LDH in the PMMA matrix, consistent with the results obtained in viscosimetric tests.

SEM micrographs were obtained for a more precise structural characterization of the LDH dispersion in the polymeric film. Figure 2 depicts the micrographs obtained for PMMA and PMMA/LDH (0.25 wt%), non-irradiated and irradiated samples.

It is possible to observe that the micrograph of the non-irradiated PMMA film (Figure 2a) exhibits some agglomeration points referred to as clusters, which are common in films produced by the casting method[11]. The irradiated films did not find clusters (Figure 2b). However, many fissures indicate the effect of radiolysis and, consequently, the degradation of PMMA. Such fissures may explain the higher number of pores and increased roughness in the films, as shown in the topographic images obtained by AFM (Figure 1).

The micrographs of non-irradiated and irradiated PMMA/LDH films exhibit a clear difference from pure PMMA samples. It is observed that LDH is homogeneously distributed in the polymeric matrix. The structure found in the PMMA/LDH samples (Figures 2c and 2d) showed a completely different cluster form, highlighting the lamellar agglomerates. These agglomerates may contribute to the increased roughness of the films with LDH, shown in Figure 1. The reduction in the roughness of the irradiated PMMA/LDH film may be associated with the production of pores with irregular structures formed by the radiolytic degradation of polymer chains (Figure 2d). However, the structural preservation of the irradiated PMMA/LDH film is evident when compared to the film without LDH (Figure 2b). This result reinforces the radioprotective action of LDH at 0.25 wt%.

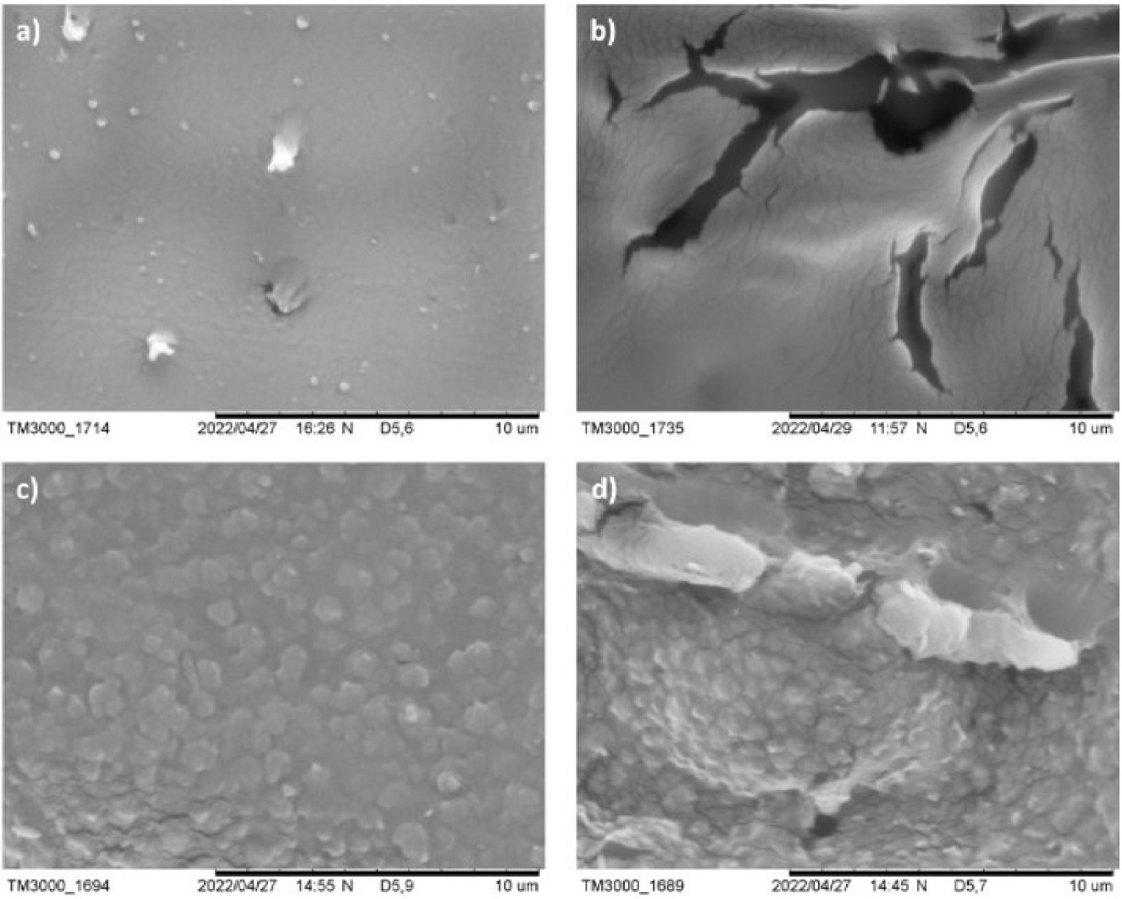

**Figure 2.** SEM images (x 10,000) for (a) PMMA 0 kGy; (b) PMMA 25 kGy; (c) PMMA/LDH 0 kGy; and (d) PMMA/LDH 25 kGy (LDH at 0.25wt%).

### *3.3 Mechanical properties*

Table 2 shows the results of the mechanical properties obtained for irradiated and non-irradiated films of PMMA and PMMA/LDH (0.25 wt%). It was observed that PMMA non-irradiated has a higher value of elastic modulus and higher tensile strength values when compared to the values obtained for PMMA/LDH. These results indicate higher stiffness of PMMA, although the polymer exhibits a higher elongation at break.

**Table 2.** Mechanical properties obtained for irradiated and non-irradiated PMMA and PMMA/LDH (0.25 wt%) films.

| Sample | Elastic modulus (Mpa) | Tensile Strength (MPa) | Elongation at break |
|---|---|---|---|
| PMMA (0 kGy) | 2395 ± 763$^{a}$ | 36 ± 5$^{a}$ | 3.0 ± 1.0$^{a}$ |
| PMMA (25 kGy) | 1551 ± 733$^{b}$ | 13 ± 6$^{b}$ | 0.9 ± 0.1$^{b}$ |
| PMMA/LDH (0 kGy) | 1485 ± 685$^{b}$ | 27 ± 6$^{c}$ | 0.6 ± 0.2$^{c}$ |
| PMMA/LDH (25 kGy) | 1871 ± 574$^{b}$ | 16 ± 8$^{b}$ | 0.7 ± 0.1$^{c}$ |

Different letters in the columns indicate a statistically significant difference at $p < 0.05$.

Changes in the elongation at break, tensile strength, and elastic modulus in non-irradiated PMMA/LDH films indicate the adhesion between the polymer and LDH phases, as these properties are sensitive to the transfer of load between the components. The elastic modulus depends on the nature of the material chemical bonding and electronic structures, while the morphology, size of domains, and film homogeneity are related to the tensile strength. The decrease in the tensile strength of PMMA/LDH films may be associated with their increased roughness (see Figure 1) and the distribution of clusters with larger sizes (see Figure 2c), causing reduced load transfer between the PMMA and LDH phases[34]. The same discussion extends to irradiated PMMA films when compared to non-irradiated samples. Figure 2b shows several fissures in the film due to main chain scissions caused by gamma radiation. Reduced load transfer is caused by radiolytic damage, creating points of force yield, causing lower tensile strength and a lower elastic modulus.

Comparing irradiated and non-irradiated PMMA/LDH films, there were no significant changes ($p < 0.05$) in the tensile strength or elongation at break. This result may be associated with the lesser damage caused by radiation to PMMA (see Figure 2d) due to the radioprotective effect of LDH. On the other hand, the decrease in tensile strength in irradiated PMMA/LDH films can be explained by the few pores and a different distribution of clusters (see Figure 2d), which reduce the interfacial interaction between PMMA and LDH, leading to a lower stress transfer at that location[34]. These results indicate that PMMA/LDH films, subjected to gamma radiation sterilization, nearly maintain their mechanical properties, strengthening the radioprotective action of LDH in the system.

### 3.4 Spectroscopic analyzes

Figure 3 shows the FT-IR spectra of PMMA and PMMA/LDH (0.25 wt%). Generally, it is possible to observe that the bands that characterize PMMA appear at a frequency similar to that of PMMA with LDH.

Figure 3a shows that the characteristic bands of PMMA appear for all studied systems (see Table S2 in Supplementary Material). Thus, the similarity between the bands or the absence of new bands, when comparing the spectra obtained for PMMA and PMMA/LDH, irradiated and non-irradiated, indicates that the nanofiller at a concentration of 0.25 wt% does not establish strong chemical bonds with the polymer. Regarding the stereoregularity of the PMMA used in this work, the absorption band in the region around 840 $cm^{-1}$ is characteristic of syndiotactic PMMA. A doublet is found in the region between 1240 and 1270 $cm^{-1}$, which is attributed to the stretching of the C-O bond in the ester group with cis conformation, which is energetically favored for syndiotactic PMMA[27].

Figure 3b shows the UV-vis spectrum for the studied films. The absorbance between 290 and 300 nm is related to the $\pi$-$\pi^*$ electronic transition. The PMMA film exhibited absorption around 285 nm, corresponding to the C=O group[35,36]. The addition of LDH did not influence the behavior of the film, but a slight shift in the absorption band was observed in the irradiated systems, with a particular emphasis on the PMMA/LDH. The increased load from the LDH and the radiolysis products may contribute to a different arrangement of molecules in the system. The optical absorption coefficient ($\alpha$) reflects the ability of material to absorb light. Figure 4a shows the intersection of the extrapolation of the linear part of the $\alpha$ versus $h\nu$ graph with the horizontal axis, providing an estimate of the photon energy absorbed by each film. Films irradiated with LDH exhibited lower energy than non-irradiated PMMA. The decrease from 4.21 eV for non-irradiated PMMA to 3.93 eV for the irradiated PMMA/LDH system provides evidence of changes in the valence and conduction band structures of the film due to the combined action of LDH and irradiation[37].

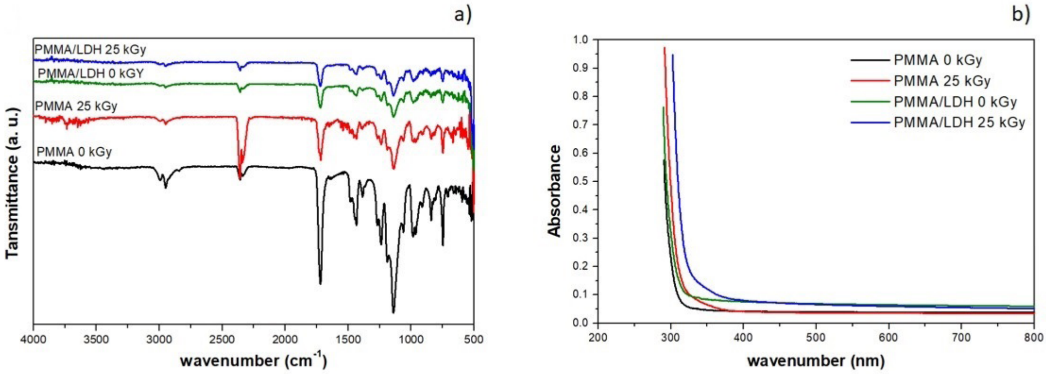

**Figure 3.** (a) FT-IR spectra for non-irradiated and irradiated PMMA and PMMA/LDH (0.25 wt%) films; and (b) UV-vis spectra for PMMA and PMMA/LDH (0.25 wt%), irradiated and non-irradiated films.

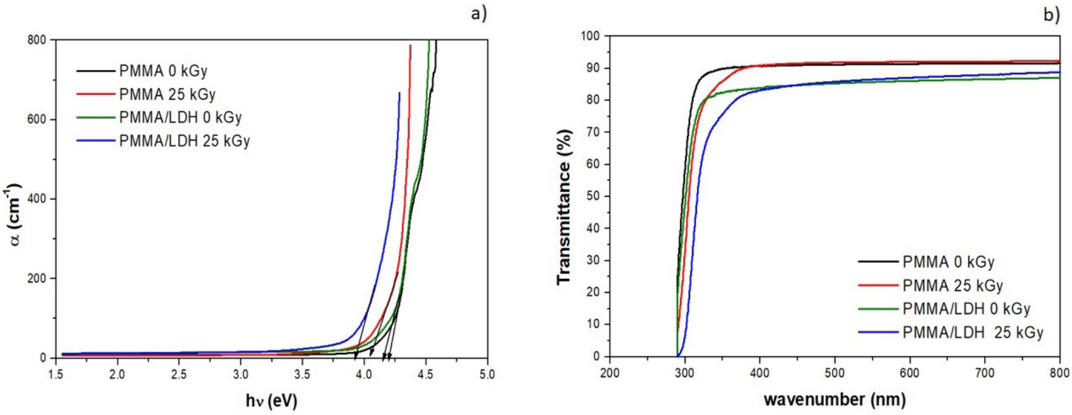

**Figure 4.** (a) Absorption coefficient ($\alpha$) for PMMA and PMMA/LDH (0.25 wt%), irradiated and non-irradiated films; and (b) Transmittance behavior of irradiated and non-irradiated PMMA and PMMA/LDH (0.25 wt%) films.

Based on the absorbance values obtained in the UV/vis spectrum (Figure 3b), the transmittance (T) calculation was performed, and the results are shown in Figure 4b. The irradiated and non-irradiated PMMA film exhibited a T value of around 90%, indicating that the irradiation process did not induce changes in this property. However, whether irradiated or non-irradiated, PMMA/LDH films showed a decrease in T of approximately 8%. This result may be associated with the increased roughness of the irradiated and non-irradiated PMMA/LDH systems (see Figure 1). Nevertheless, no significant differences were found in the refractive index ($n$) of the films. The n value was 1.36 for PMMA (irradiated and non-irradiated) and 1.37 for PMMA/LDH (irradiated and non-irradiated) at 500 nm.

The dielectric constant of the studied films, both in the real part (Figure 5a) and the imaginary part (Figure 5b), increases with the photon energy. The real part ($\varepsilon r$) is related to the speed of light and the electronic polarization of a material, while the imaginary part ($\varepsilon i$) indicates dipolar movement due to energy absorption generated by an electric field[38]. In Figure 5a the extrapolation of the linear portion of the curves with the x-axis showed the lowest photon energy is absorbed in the irradiated PMMA/LDH system. This behavior can be explained by the presence of charges from LDH and defects caused by irradiation in the PMMA matrix, albeit smaller than in the LDH-free film (see Figure 2), forming dipoles that govern the dielectric properties of the irradiated films[39].

The combined effect of LDH and irradiation also impacted the optical gap (Eg) of the films. Figure 6 shows a reduction in Eg for LDH-containing systems, particularly in the irradiated film. $E_{g,}$ values were obtained using the Tauc' s model[40] and compared with the energy obtained from the $\varepsilon i$ parameter

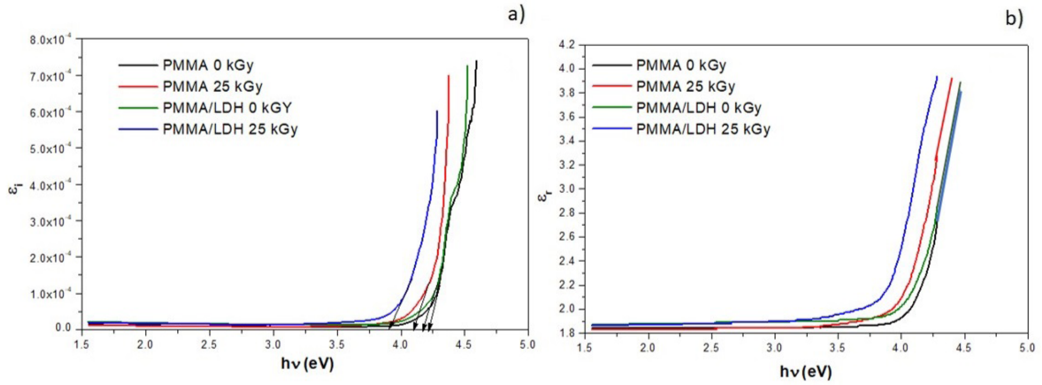

**Figure 5.** The behavior of the dielectric constant (a) imaginary part and (b) real part for PMMA and PMMA/LDH (0.25 wt%), irradiated and non-irradiated films.

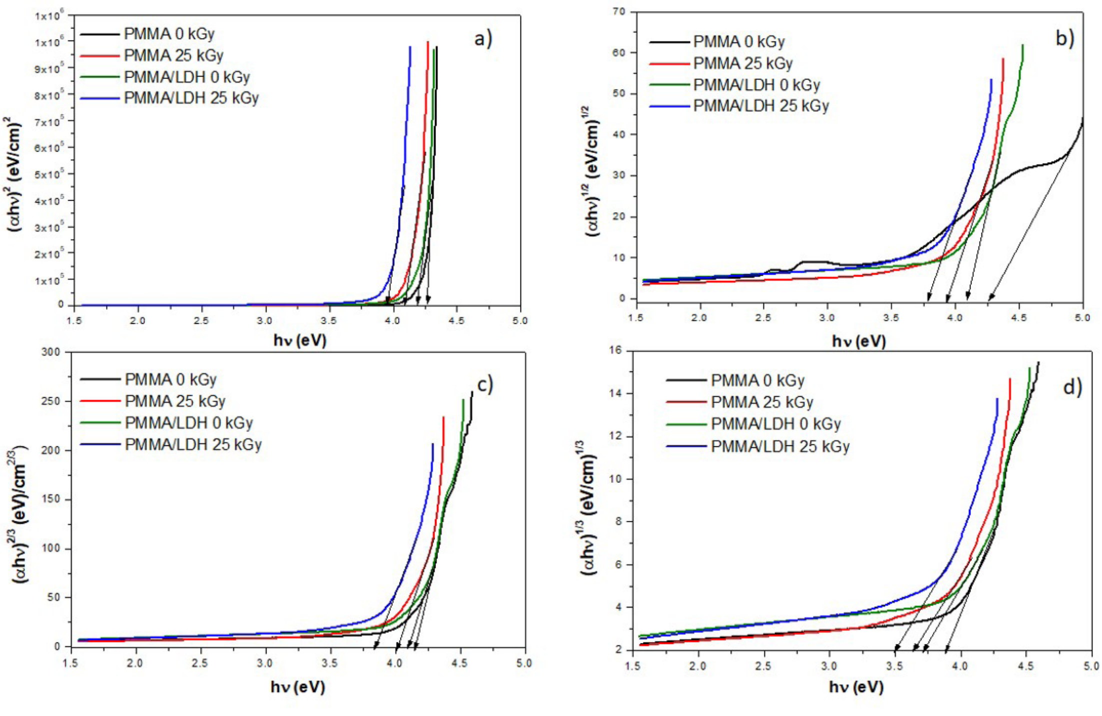

**Figure 6.** Optical gap energy obtained by the Tauc's model for (a) allowed direct transition; (b) allowed indirect transition; (c) forbidden direct transition; and (d) forbidden indirect transition.

(Figure 5a) to identify the predominant electronic transition in the systems. Table S3 (Supplementary Material) shows the $E_g$ values obtained through both methods. The results suggest that the predominant electronic transition in all systems is the allowed direct transition, given the similarity of values for this transition obtained by the Tauc method and $\varepsilon i$.

The result suggests that the electronic structure of the PMMA film undergoes changes when LDH is introduced, when it is irradiated, and especially when there is a combined effect of LDH and irradiation. These electronic changes may promote a different band arrangement capable of reducing the energy required for an electron to move from the valence band to the conduction band[41]. This finding is consistent with the discussion regarding the optical absorption coefficient (α), where lower energies for LDH-containing and irradiated systems were identified through the graph in Figure 4a.

On the other hand, optical conductivity ($\sigma_{opt}$) informs about the movement of charge carriers when excited by incident electromagnetic radiation. The influence of LDH and irradiation on the $\sigma_{opt}$ of the films is shown in Figure 7. The values of $\sigma_{opt}$ decrease with the increase in wavelength, but no significant changes are observed in the maximum value of $\sigma_{opt}$ for the films. However, the curve of the irradiated PMMA/LDH system is shifted towards a longer wavelength, which may be due to new levels within the band gap. New levels facilitate the movement of electrons from the valence band to the conduction band due to increased photon-atom interaction[42]. This result corroborates with the lower $E_g$ found for irradiated PMMA/LDH (see Table S3 in Supplementary Material) and highlights the influence of the combined effect of LDH and gamma irradiation on the polymeric system.

## 4. Conclusion

In this study, nanoscale magnesium LDH was synthesized and incorporated into the PMMA matrix through in situ polymerization. Viscosimetric assays revealed that Mg-LDH 0.25 wt% acts as a radioprotector in the PMMA matrix exposed to gamma radiation at a dose of 25 kGy. In this way, LDH provided approximately 90% protection against the chain scission effect caused by radiolysis in the main PMMA chain, probably as a scavenger agent.

Characterization of irradiated and non-irradiated PMMA/LDH (0.25 wt%) films reveals that the combined effect of LDH and gamma radiation induces changes in the polymeric system structure. SEM images confirmed the damaging effect of radiation on PMMA while also revealing the homogeneous distribution of nanofillers in the system and the more preserved appearance of the irradiated LDH-containing film. Moreover, the higher roughness of the PMMA/LDH system decreased the film transmittance by 8% for both irradiated and non-irradiated conditions. The FT-IR spectra did not show new bands or shifts when comparing systems with and without LDH. These results indicate that there are no strong chemical bonds between PMMA and LDH and that PMMA/LDH films exposed to gamma radiation practically maintain their mechanical properties, reinforcing the radioprotective action of LDH in the system. The UV-vis analysis revealed that PMMA and PMMA/LDH films (irradiated and non-irradiated) absorb energy around 290 nm, attributed to the π-electron transition of the carbonyl group.

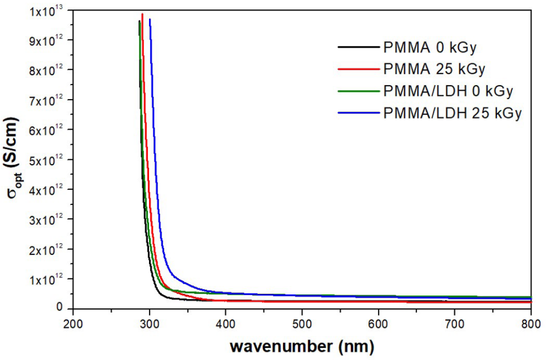

**Figure 7.** The behavior of optical conductivity ($\sigma_{opt}$) for PMMA and PMMA/LDH (0.25 wt%), irradiated and non-irradiated films.

Thus, the optical parameters were also influenced by the combined effect of LDH and gamma irradiation. The optical conductivity and dielectric constant values remained the same, with peak values associated with lower energies in the irradiated and LDH-containing systems. The impact of this behavior was to decrease the optical gap value of irradiated PMMA/LDH films. These results indicate that the optical properties of PMMA/LDH films can be modulated under gamma irradiation.

## 5. Author's Contribution

- **Conceptualization** – Kátia Aparecida da Silva Aquino.
- **Data curation** – Dandara Luz Souza de Oliveira, Amanda Damasceno Leão.
- **Formal analysis** – Dandara Luz Souza de Oliveira, Amanda Damasceno Leão.
- **Funding acquisition** – Kátia Aparecida da Silva Aquino.
- **Investigation** – Kátia Aparecida da Silva Aquino.
- **Methodology** – Dandara Luz Souza de Oliveira; Amanda Damasceno Leão; Pietro Paolo Jorge Correia de Oliveira e Silva; Fábio de Oliveira da Silva Ribeiro, Alyne Rodrigues de Araújo Silva.
- **Project administration** – Kátia Aparecida da Silva Aquino.
- **Resources** – Elmo Silvano de Araújo; Renata Francisca da Silva Santos, Kátia Aparecida da Silva Aquino.
- **Software** – Fábio de Oliveira da Silva Ribeiro; Alyne Rodrigues de Araújo.
- **Supervision** – Elmo Silvano de Araújo; Kátia Aparecida da Silva Aquino.
- **Validation** – Kátia Aparecida da Silva Aquino; José Lamartine Soares-Sobrinho.
- **Visualization** – Kátia Aparecida da Silva Aquino; José Lamartine Soares-Sobrinho.
- **Writing – original draft** – Dandara Luz Souza de Oliveira; Amanda Damasceno Leão.
- **Writing – review & editing** – Kátia Aparecida da Silva Aquino.

## 6. Acknowledgements

This project was supported by the Brazilian Federal Agency for Support and Evaluation of Graduate Education (CAPES). The authors also thank the Laboratory of Phytochemistry and Process Integration-LAFIP (CETENE-Brazil) for its support in experimental activities.

## 7. References

1. Leão, A. D., França, L. M., Cunha, C. N. L. C., Marinho, F. A., Soares, M. F. L., & Soares-Sobrinho, J. L. (2019). In-line monitoring of layered double hydroxide synthesis and insights on formation mechanism and kinetics. *Applied Clay Science*, *179*, 105130. http://doi.org/10.1016/j.clay.2019.105130.
2. Leão, A. D., Alvarez-Lorenzo, C., & Soares-Sobrinho, J. L. (2020). One-pot synthesis of the organomodified layered double hydroxides - glibenclamide biocompatible nanoparticles. *Colloids and Surfaces. B, Biointerfaces*, *193*, 111055. http://doi.org/10.1016/j.colsurfb.2020.111055. PMid:32403034.
3. Nagendra, B., Mohan, K., & Gowd, E. B. (2015). Polypropylene/layered double hydroxide (LDH) nanocomposites: influence of LDH particle size on the crystallization behavior of polypropylene. *ACS Applied Materials & Interfaces*, *7*(23), 12399-12410. http://doi.org/10.1021/am5075826. PMid:25741910.
4. Hoxha, A., Gillam, D. G., Agha, A., Karpukhina, N., Bushby, A. J., & Patel, M. P. (2020). Novel fluoride rechargeable dental composites containing MgAl and CaAl layered double hydroxide (LDH). *Dental Materials*, *36*(8), 973-986. http://doi.org/10.1016/j.dental.2020.04.011. PMid:32536588.
5. Manzi-Nshuti, C., Wang, D., Hossenlopp, J. M., & Wilkie, C. A. (2008). Aluminum-containing layered double hydroxides: the thermal, mechanical, and fire properties of (nano)composites of poly(methyl methacrylate). *Journal of Materials Chemistry*, *18*(26), 3091-3102. http://doi.org/10.1039/b802553c.
6. Charlesby, A. (1960). *Atomic radiation and polymers*. Oxford: Pergamon Press. http://doi.org/10.1016/C2013-0-07861-9.
7. Aquino, K. A. S., Araújo, E. S., & Guedes, S. M. L. (2010). Influence of a hindered amine stabilizer on optical and mechanical properties of poly(methyl methacrylate) exposed to gamma irradiation. *Journal of Applied Polymer Science*, *116*(2), 748-753. http://doi.org/10.1002/app.31544.
8. Garcia, O. P., Albuquerque, M. C. C., Aquino, K. A. S., Araujo, P. L. B., & Araujo, E. S. (2015). Use of lead (II) sulfide nanoparticles as stabilizer for PMMA exposed to gamma irradiation. *Materials Research*, *18*(2), 365-372. http://doi.org/10.1590/1516-1439.330214.
9. Albuquerque, M. C. C., Garcia, O. P., Aquino, K. A. D. S., Araujo, P. L. B., & Araujo, E. S. (2015). Stibnite nanoparticles as a new stabilizer for poly(methyl methacrylate) exposed to gamma irradiation. *Materials Research*, *18*(5), 978-983. http://doi.org/10.1590/1516-1439.000814.
10. Chen, H., Mousty, C., Cosnier, S., Silveira, C., Moura, J. J. G., & Almeida, M. G. (2007). Highly sensitive nitrite biosensor based on the electrical wiring of nitrite reductase by [ZnCr-AQS] LDH. *Electrochemistry Communications*, *9*(9), 2240-2245. http://doi.org/10.1016/j.elecom.2007.05.030.
11. Leão, A. D., Silva, L. A., Ribeiro, F. O. S., Silva, D. A., França, E. J., Aquino, K. A. S., & Soares-Sobrinho, J. L. (2021). Influence of nonmodified layered double hydroxide (LDH) metal constituents in PMMA/LDH nanocomposites. *Journal of Inorganic and Organometallic Polymers and Materials*, *31*(2), 836-850. http://doi.org/10.1007/s10904-020-01742-z.
12. Lu, X., Wang, C., & Wei, Y. (2009). One-dimensional composite nanomaterials: synthesis by electrospinning and their applications. *Small*, *5*(21), 2349-2370. http://doi.org/10.1002/smll.200900445. PMid:19771565.
13. Ding, Y., Gui, Z., Zhu, J., Hu, Y., & Wang, Z. (2008). Exfoliated poly(methyl methacrylate)/MgFe-layered double hydroxide nanocomposites with small inorganic loading and enhanced properties. *Materials Research Bulletin*, *43*(12), 3212-3220. http://doi.org/10.1016/j.materresbull.2008.03.002.
14. Wang, Q., Undrell, J. P., Gao, Y., Cai, G., Buffet, J.-C., Wilkie, C. A., & O'Hare, D. (2013). Synthesis of flame-retardant polypropylene/LDH borate nanocomposites. *Macromolecules*, *46*(15), 6145-6150. http://doi.org/10.1021/ma401133s.
15. Demir, M. M., Memesa, M., Castignolles, P., & Wegner, G. (2006). PMMA/Zinc oxide nanocomposites prepared by in-situ bulk polymerization. *Macromolecular Rapid Communications*, *27*(10), 763-770. http://doi.org/10.1002/marc.200500870.
16. Li, B., Hu, Y., Liu, J., Chen, Z., & Fan, W. (2003). Preparation of poly(methyl methacrylate)/LDH nanocomposite by exfoliation-adsorption process. *Colloid & Polymer Science*, *281*(10), 998-1001. http://doi.org/10.1007/s00396-003-0874-5.
17. Miyata, S., & Okada, A. (1977). Synthesis of hydrotalcite-like compounds and their physico-chemical properties– the systems $Mg^{2+}$-$Al^{3+}$-$SO_2^-$ and $Mg^{2+}$-$Al^{3+}$-$CrO_2^-$. *Clays and Clay Minerals*, *25*(1), 14-18. http://doi.org/10.1346/CCMN.1977.0250103.
18. Mayo-Pedrosa, M., Alvarez-Lorenzo, C., Lacík, I., Martinez-Pacheco, R., & Concheiro, A. (2007). Sustained release pellets based on poly(N-isopropyl acrylamide): matrix and in situ photopolymerization-coated systems. *Journal of Pharmaceutical Sciences*, *96*(1), 93-105. http://doi.org/10.1002/jps.20708. PMid:16967440.
19. Schoff, C. K. (1999). *Concentration dependence of the viscosity of dilute polymer solutions: Huggins and Schulz-Blaschke constants.* In J. Brandrup, E. H. Immergut & E. A. Grulke (Eds.), *Polymer handbook* (pp. 265-289). New York: Wiley-Interscience. http://doi.org/10.1002/0471532053.bra053.
20. Huggins, M. L. (1942). The viscosity of dilute solutions of long-chain molecules. IV. Dependence on concentration. *Journal of the American Chemical Society*, *64*(11), 2716-2718. http://doi.org/10.1021/ja01263a056.
21. Solomon, O. F., & Ciută, I. Z. (1962). Détermination de la viscosité intrinsèque de solutions de polymères par une simple détermination de la viscosité. *Journal of Applied Polymer Science*, *6*(24), 683-686. http://doi.org/10.1002/app.1962.070062414.
22. Qian, J. W., Qi, G. R., & Cheng, R. S. (1997). Association of ethylene-vinylacetate copolymer in dilute solutions-I. Solvent, concentration and annealing temperature effect. *European Polymer Journal*, *33*(8), 1263-1265. http://doi.org/10.1016/S0014-3057(96)00264-9.
23. Ubale, A. U., Sangawar, V. S., & Kulkarni, D. K. (2007). Size dependent optical characteristics of chemically deposited nanostructured ZnS thin films. *Bulletin of Materials Science*, *30*(2), 147-151. http://doi.org/10.1007/s12034-007-0026-5.
24. Davis, E. A., & Mott, N. F. (1970). Conduction in non-crystalline systems V. Conductivity, optical absorption and photoconductivity in amorphous semiconductors. *Philosophical Magazine*, *22*(179), 903-922. http://doi.org/10.1080/14786437008221061.
25. Guo, M., & Du, J. (2012). First-principles study of electronic structures and optical properties of Cu, Ag, and Au-doped anatase $TiO_2$. *Physica B, Condensed Matter*, *407*(6), 1003-1007. http://doi.org/10.1016/j.physb.2011.12.128.
26. Pankove, J. I., & Kiewit, D. A. (1972). Optical processes in semiconductors. *Journal of the Electrochemical Society*, *119*(5), 156C. http://doi.org/10.1149/1.2404256.
27. Booth, H. (1992). Review of *Spectrometric identification of organic compounds*, by R. M. Silverstein, G. C. Bassler, & T. C. Morrill. *Magnetic Resonance in Chemistry*, *30*(4), 364. http://doi.org/10.1002/mrc.1260300417.

28. Guillet, J. E. (Ed.). (1985). *Polymer photophysics and photochemistry: an introduction to the study of photoprocesses in macromolecules*. Cambridge: Cambridge University Press. http://doi.org/10.1002/zfch.19860261131.
29. Brandrup, J., & Immergut, E. H. (Eds.). (1989). *Polymer handbook*. New York: Wiley-Interscience. http://doi.org/10.1002/actp.1990.010410614.
30. Lovell, P. A. (1989). *Dilute solution viscometry.* In G. Allen & J. C. Bevington (Eds.), *Comprehensive polymer science and supplements* (pp. 173-197). New York: Elsevier. http://doi.org/10.1016/B978-0-08-096701-1.00009-4.
31. Bel, T., Arslan, C., & Baydogan, N. (2019). Radiation shielding properties of poly (methyl methacrylate) / colemanite composite for the use in mixed irradiation fields of neutrons and gamma rays. *Materials Chemistry and Physics*, *221*, 58-67. http://doi.org/10.1016/j.matchemphys.2018.09.014.
32. Aquino, K. A. S., & Araújo, E. S. (2008). Effects of a hindered amine stabilizer (HAS) on radiolytic and thermal stability of poly (methyl methacrylate). *Journal of Applied Polymer Science*, *110*(1), 401-407. http://doi.org/10.1002/app.28465.
33. Aquino, K. A. S., Oliveira, D. L. S., Santos, R. F. S., & Araújo, E. S. (2023). Study of commercial additive effects on poly(methyl methacrylate) exposed to gamma irradiation by viscosimetric analysis. *Materials Research*, *26*, e20230382. http://doi.org/10.1590/1980-5373-mr-2023-0382.
34. Koning, C., Duin, M. V., Pagnoulle, C., & Jerome, R. (1998). Strategies for compatibilization of polymer blends. *Progress in Polymer Science*, *23*(4), 707-757. http://doi.org/10.1016/S0079-6700(97)00054-3.
35. Wang, X., Huang, J., Fan, W., & Lu, H. (2015). Identification of green tea varieties and fast quantification of total polyphenols by near-infrared spectroscopy and ultraviolet-visible spectroscopy with chemometric algorithms. *Analytical Methods*, *7*(7), 787-792. http://doi.org/10.1039/C4AY02106A.
36. Al-Kadhemy, M. F. H., Saeed, A. A., Khaleel, R. I., & Al-Nuaimi, F. J. K. (2017). Effect of gamma ray on optical characteristics of (PMMA/PS) polymer blends. *Journal of Theoretical and Applied Physics*, *11*(3), 201-207. http://doi.org/10.1007/s40094-017-0259-7.
37. Aziz, S. B., Rasheed, M. A., Hussein, A. M., & Ahmed, H. M. (2017). Fabrication of polymer blend composites based on PVA-PVP:$(Ag_2S)x$ $(0.01 \leq x \leq 0.03)$ with small optical band gaps: structural and optical properties. *Materials Science in Semiconductor Processing*, *71*, 197-203. http://doi.org/10.1016/j.mssp.2017.05.035.
38. Omar, M. A. (1987). *Elementary solid state physics: principles and applications*. Reading: Addison-Wesley Publishing Company.
39. Tahir, K. J. (2017). Effect of gamma irradiation on optical properties of CdS thin films. *Journal of Kerbala University*, *15*(1), 49-55. Retrieved in 2024, August 13, from https://www.iasj.net/iasj/article/122592
40. Tauc, J. (Ed.). (1974). *Amorphous and liquid semiconductors*. London: Plenum Publishing Company Ltd. http://doi.org/10.1007/978-1-4615-8705-7.
41. Ersen, Y. (2022). Compatibilizer effect on optical properties of immiscible PMMA/PS blends. *International Journal of Pure and Applied Sciences*, *8*(1), 149-156. http://doi.org/10.29132/ijpas.1054866.
42. Mansour, A. F., Mansour, S. F., & Abdo, M. A. (2015). Improvement of structural and optical properties of ZnO/PVA nanocomposites. *IOSR Journal of Applied Physics*, *7*(2), 60-69. http://doi.org/10.9790/4861-07226069.

*Received: Aug. 13, 2024*
*Revised: Oct. 21, 2024*
*Accepted: Oct. 29, 2024*

## Supplementary Material

Supplementary material accompanies this paper.

Table S1. Viscosimetric parameters and their mathematical relationships.

Table S2. Band assignment in the FT-IR spectrum of PMMA. Adapted from Booth et al.[11].

Table S3. Eg values obtained through the Tauc's model and from the parameter $\varepsilon i$.

Figure S1. SEM micrograph (x50,000) of the magnesium LDH synthesized for this study.

Figure S2. Reduced viscosity vs concentration for non-irradiated PMMA solutions.

This material is available as part of the online article from https://doi.org/10.1590/0104-1428.20240077